Novel and potent Dengue virus NS2B/NS3 protease inhibitors

Hongmei Wu, Stefanie Bock, Mariya Snitko, Thilo Berger, Thomas Weidner, Steven Holloway, Manuel Kanitz, Wibke E. Diederich, Holger Steuber, Christof Walter, Daniela Hofmann, Benedikt Weißbrich, Ralf Spannaus, Eliana G. Acosta, Ralf Bartenschlager, Bernd Engels, Tanja Schirmeister and Jochen Bodem

Supplementary Information

Contents:

Chemistry

All chemicals and solvents were obtained at analytical grade from Sigma-Aldrich (Germany), abcr (Germany), Iris Biotech and Alfa Aesar. Solvents were dried using standard procedures. Melting points were determined on a Stuart SMP10 apparatus. *Infrared spectra (IR) were recorded* on an *Avatar 330* FT-IR *Thermo Nicolet* spectrophotometer. Field desorption (FD) mass spectra were performed with a *VG-Instruments ZAB 2-SE-FDP* instrument. ^{1}H and ^{13}C spectra were recorded on a Bruker Avance 400 (400 MHz) or Bruker Fourier 300 (300 MHz) at 300 K in $CDCl_3$, DMSO-d_6. Chemical shifts are given in parts per million (δ, ppm) and the residuals of non-deuterated solvents were used as internal standard (^{1}H NMR: $CDCl_3$: δ = 7.26 ppm, DMSO-d_6: δ = 2.50 ppm, ^{13}C NMR: $CDCl_3$: δ = 77.16 ppm, DMSO-d_6: δ = 39.52 ppm). Coupling con-

stants (*J*) are given in Hertz (Hz). Multiplicity is reported as s (singlet), d (doublet), t (triplet), dd (doublet-doublet), dt (doublet-triplet), td (triplet-doublet), m (multiplet) and br (broad), respectively. Chromatography was performed using silica gel (0.060–0.200 mm) and UV monitoring. Reaction progress was determined by thin layer chromatography on Merck Silica Gel plates 60 F254 (UV detection). The purity of the compounds was determined by analytic HPLC (Waters®HPLC) with Diode Array Detector (DAD) using an Orbit 250 x 4,6 mm; 100 C18 5µm column. The analysis was performed using a solvent gradient conducted from 5% to 95% acetonitrile over water in 20 minutes with a flow rate of 1 ml/min.

Synthesis of intermediate I1:

To a solution of 2-mercaptobenzoic acid (1.54 g, 10 mmol) in 30 ml ethanol ethanolic sodium ethoxide (25 ml, 2%) was added under stirring (Figure S1). The solvent was then evaporated under reduced pressure. The resulting residue was dissolved in dimethylformamide (30 ml) and *p*-chloronitrobenzene (1.8 g, 11.4 mmol) was added to the solution. The reaction mixture was reflux for 6 hours. After cooling to room temperature, water was added under continuous stirring. The resulting precipitate was filtered off and dissolved in aqueous potassium carbonate solution (50 ml, 5%). The solution was washed with chloroform to remove excess *p*-chloronitrobenzene. The aqueous phase was neutralized with hydrochloric acid. The resulting precipitate was filtered, washed with methanol and dried to yield 2-(4-nitrophenylthio)-benzoic acid **I1** in 77% (2.1 g) yield [1].

Synthesis of 1:

To a solution of 2-(4-nitrophenylthio)-benzoic acid (**I1**, 82.6 mg, 0.3 mmol) (Supplementary Figure S1), HBTU (136.5 mg, 0.36 mmol) and *N*-methylmorpholine (0.12 ml) in DMF 2-thiophenamine (31.2 mg, 0.32 mmol) was added (Figure S1). After stirring at room temperature under argon atmosphere overnight, water was added. The mixture was extracted 3 times with

CH_2Cl_2, dried over anhydrous Na_2SO_4, filtered, and the solvent was evaporated under reduced pressure. Compound **1** was obtained after chromatography as a yellow solid (35 mg, 33%) (Figure S1).

^{1}H-NMR ($CDCl_3$, 400 MHz), δ [ppm] = 8.93 (s, 1 H), 8.07 (d, ^3J = 8.9 Hz, 2 H), 7.94 – 7.91 (m, 1 H), 7.60 – 7.52 (m, 3H), 7.27 (d, ^3J = 9.5 Hz, 2 H), 6.91 (dd, ^3J = 5.5 Hz, ^4J = 0.9 Hz, 1 H), 6.86 (dd, ^3J = 5.5 Hz, ^3J = 3.8 Hz, 1 H), 6.68 (dd, ^3J = 3.7 Hz, ^4J = 1.3 Hz, 1 H).

^{13}C-NMR ($CDCl_3$, 101MHz), δ [ppm] = 163.26, 146.44, 145.51, 138.54, 137.83, 136.02, 132.27, 130.63, 130.12, 129.73, 128.64, 124.51, 124.20, 118.83, 112.83.

FT-IR: $\tilde{\nu}$ [cm^{-1}] = 3244, 3101, 2921, 2852, 1633, 1579, 1557, 1502, 1336, 1309, 736, 695.

Melting point: 136 °C

FD-MS: [M] 356.0

Purity: 96%

Synthesis of 2:

To a solution of 2-(4-nitrophenylthio)-benzoic acid (**I1**, 165.0 mg, 0.6 mmol), HBTU (250.3 mg, 0.66 mmol) and *N*-methylmorpholine (0.24 ml) in DMF 2-amino-6-nitrobenzothiazole (128.8 mg, 0.66 mmol) was added (Figure S1). After stirring at room temperature under argon atmosphere overnight, water was added. The precipitate was collected by filtration and washed with water. The obtained crude compound was purified by chromatography to yield compound **2** as a yellow solid (50 mg, 19%) (Supplementary Figure S1).

^{1}H-NMR (400 MHz, DMSO-d_6), δ [ppm] =13.39 (s, 1H), 9.08 (d, ^4J = 2.4 Hz, 1H), 8.30 (dd, ^3J = 9.0 Hz, ^4J = 2.4 Hz, 1H), 8.16 – 8.10 (m, 2H), 7.92 (d, ^3J = 9.0 Hz, 1H), 7.90 – 7.85 (m, 1H), 7.69 – 7.57 (m, 3H), 7.41 – 7.34 (m, 2H).

^{13}C-NMR (101 MHz, DMSO-d_6), δ [ppm] = 167.14, 163.44, 153.32, 145.97, 145.62, 143.18, 137.72, 134.81, 132.44, 132.23, 130.05, 129.45, 129.41, 128.90 (2C), 124.29 (2C), 121.89, 120.82, 119.19.

FT-IR: $\tilde{\nu}$ [cm^{-1}] = 3224, 3162, 3097, 2945, 2844, 1683, 1573, 1502, 1336, 1262, 1242.

Melting point: 253 °C

FD-MS: [M] 452.8

Purity: 99%

Synthesis of intermediate I2:

A mixture of 2-mercaptobenzoic acid (1.0 g, 6.5 mmol), sodium hydroxide (0.6 g, 15.0 mmol) and 1-chloro-4-(trifluoromethyl)benzene (1.6 g, 8.86 mmol) in 6 ml DMF was heated under reflux for 20 hours (Figure S1). After cooling to room temperature, the mixture was poured into water (15 ml) with stirring. Then 1 M aqueous hydrochloride solution was added to the mixture and a pH of 2-3 was adjusted. The resulting precipitate was filtered, washed with water and dried to give **I2** in 13% (300 mg) yield (Supplementary Figure S1).

Synthesis of 3:

In the same manner as that described for the preparation of **2**, starting from 2-[[4-(trifluoromethyl)phenyl]thio]-benzoic acid (**I2**, 179.0 mg, 0.6 mmol) and 2-amino-6-nitrobenzothiazole (128.8 mg, 0.66 mmol), compound **3** was obtained after precipitation and chromatography as a white powder (87.8 mg, 31%) (Supplementary Fig. 1).

^{1}H-NMR (400 MHz, $CDCl_3$) δ [ppm] = 11.58 (s, 1H), 8.76 (d, ^{4}J = 2.2 Hz, 1H), 8.16 (dd, ^{3}J = 8.9, ^{4}J = 2.2 Hz, 1H), 7.94 (dd, ^{3}J = 7.5 Hz, ^{4}J =1.7 Hz, 1H), 7.53 – 7.41 (m, 4H), 7.35 – 7.33 (m, 4H).

^{13}C-NMR (75 MHz, DMSO-d_6) δ [ppm] = 167.23, 163.60, 153.28, 143.14, 141.12, 136.33, 133.27, 132.37, 132.25, 130.45 (2C), 129.28, 128.30, 127.41(q, J = 31,9Hz), 127.20, 126.19 (q, 2C, J = 3.7 Hz), 124.05 (q, J = 272.2Hz), 121.83, 120.71, 119.13.

FT-IR: $\tilde{\nu}$ [cm^{-1}] = 3097, 2933, 1679, 1507, 1336, 1295, 1123, 1058.

Melting point: 198 °C

FD-MS: [M] 475.2

Purity: 99%

Synthesis of intermediate I3:

Same procedure as that described for the preparation of compound **I1**. Starting from 3-mercaptobenzoic acid (1.29 g, 8.2 mmol), and *p*-chloronitrobenzene (1.1 g, 7.2 mmol), compound **I3** was obtained as a yellow solid (1.06 g, 53%).

Synthesis of 4:

In the same manner as that described for the preparation of **2**, starting from 3-(4-nitrophenylthio)-benzoic acid (**I3**, 275.3 mg, 1.0 mmol) and 2-amino-6-nitrobenzothiazole (214.7 mg, 1.1 mmol) **4** was obtained after precipitation and chromatography (dichlormethane) as yellow solid (105 mg, 23%) (Supplementary Figure 1).

^{1}H-NMR (400 MHz, DMSO-d_6) δ [ppm] = 13.43 (s, 1H), 9.11 (d, *J* = 2.3 Hz, 1H), 8.38 (t, *J* = 1.6 Hz, 1H), 8.32 (dd, *J* = 8.9, 2.4 Hz, 1H), 8.29 – 8.23 (m, 1H), 8.21 – 8.15 (m, 2H), 7.94 (d, *J* = 8.9 Hz, 1H), 7.88 (ddd, *J* = 7.7, 1.7, 1.1 Hz, 1H), 7.74 (t, *J* = 7.8 Hz, 1H), 7.45 – 7.38 (m, 2H), 7.44 – 7.39 (m, 1H).

^{13}C-NMR (75 MHz, DMSO-d_6) δ [ppm] = 165.57, 164.30, 153.27, 146.34, 145.43, 143.16, 138.50, 133.90, 133.39, 132.23, 131.13, 130.72, 129.74, 127.72 (2C), 124.42 (2C), 121.87, 120.60, 119.16.

FT-IR: $\tilde{\nu}$ [cm^{-1}] = 3154, 3117, 3072, 2913, 1675, 1573, 1336, 1262, 1242, 726.

Melting point: 241 °C

FD-MS: [M] 452.8

Purity: 99%

Synthesis of intermediate I4:

To a suspension of methyl-4-amino-2-methoxybenzoate (1.5 g, 8.28 mmol), potassium thiocyanate (3.25 g, 33.44 mmol) in 15 ml acetic acid, bromine (1.33 g, 8.32 mmol) was added drop-

wise at room temperature (Figure S1). After stirring at room temperature overnight, the suspension was subsequently incubated at 60 °C overnight followed by stirring at room temperature overnight. The suspension was concentrated, the solid was poured into a half saturated $NaHCO_3$ solution and stirred for 30 minutes. The suspension was filtered off, the solid was washed with water and dried to afford 2-amino-5-methoxy-benzothiazole-6-caboxylic acid methyl ester **4** 1.55 g (79% yield) (Supplementary Figure 1).

Synthesis of intermediate I5:

In the same manner as that described for the preparation of **2**, starting from 2-[[4-(trifluoromethyl)phenyl]thio]-benzoic acid (**I2**, 298.3 mg, 1 mmol) and compound **I4** (262.0 mg, 1.1 mmol), intermediate **I5** was obtained after precipitation and chromatography as solid (346 mg, 67%) (Supplementary Figure S2).

Synthesis of 5:

An excessive amount (0.4 ml, 0.4 mmol) of a solution of boron tribromide (1M in dichloromethane) was added dropwise to a solution of 103.7 mg (0.2 mmol) of intermediate **I5** in 5 ml of dry dichloromethane at -78 °C. The reaction mixture was stirred for 24 hours and then quenched with water at room temperature. After extraction with dichloromethane and ethyl acetate the combined organic layers were dried over sodium sulfate, filtered and the solvents removed *in vacuo* [2]. The crude product was purified via column chromatography and recrystallized with ethyl acetate/ methanol and gave 170 mg (0.368 mmol, 46%) of the desired product **5** as a white powder (Supplementary Figure S1).

^{1}H-NMR (400 MHz, DMSO-d_6) δ [ppm] = 13.08 (br, 2H), 8.47 (s, 1H), 7.82 (dd, *J* = 7.4, 1.5 Hz, 1H), 7.68 (d, *J* = 8.4 Hz, 2H), 7.61 – 7.49 (m, 2H), 7.44 (m, 3H), 7.21 (s, 1H).

^{13}C-NMR (101 MHz, DMSO-d_6) δ [ppm] =171.71, 170.32, 159.97, 141.21, 136.64, 133.22, 132.27, 132.10, 130.41 (2C), 129.17, 128.26, 127.22, 126.16 (2C), 125.41, 124.40, 122.71, 122.42, 110.55, 106.69.

FT-IR: $\tilde{\nu}$ [cm^{-1}] = 3253, 3154, 2950, 2355, 1683, 1602, 1320, 1252.

Melting point: 285 °C

FD-MS: [M] 490

Purity: 99%

Synthesis of intermediate I6:

A mixture of 2-iodbenzoic acid (248.0 mg, 1mmol), 6-methoxy-2-naphthol (174.2 mg, 1 mmol), K_2CO_3 (276.4 mg, 2 mmol), Cu powder (63.6 mg, 1 mmol) in 5 ml xylene was kept at reflux for 8 h [3]. After cooling to room temperature, water was added and the mixture was acidified with 1 M aqueous hydrochloride and extracted with ethyl acetate three times, dried over anhydrous Na_2SO_4 and filtered off (Supplementary Figure S2). The solvent was evaporated under reduced pressure. After purification by chromatography (silica gel, petro ether/EtOAc = 2/1 with 0.1% formic acid) the product could be obtained as an off-white solid (107 mg, 36%) (Figure S2).
^{1}H-NMR (300 MHz, DMSO-d_6), δ [ppm] = 7.84 (m, 2H), 7.71 (d, J=9.0 Hz, 1 H), 7.60-7.51 (m, 1H), 7.26 (m, 4H), 7.13 (dd, J= 9.0, 2.4 Hz, 1H), 7.03 (d, J= 8.2 HZ, 1H), 3.85 (s, 3H)

Synthesis of intemediate I7:

A solution of 1.0 eq. of bromine (1.5 ml, 29.276 mmol) in 20 ml of glacial acetic acid was added drop-wise to a solution of 1.0 eq. (4.600 g, 30 mmol) of 3,4-dimethoxyaniline and 4.0 eq. (11.7 g, 120 mmol) of potassium thiocyanate in 40 ml of glacial acetic acid at room temperature (Supplementary Figure S1). If heating occurred, the reaction was temporarily cooled in an ice water bath (0 °C) and then stirred at room temperature for at least 10 hours (overnight). The reaction mixture was filtered and the filter residue washed with water. The filtrate solution were combined

and neutralized with concentrated aqueous ammonia solution (26%). The precipitate was filtered off, washed with water, dried *in vacuo* and finally gave rise to the desired product **I7** [4] as a dark purple, crystalline powder which was used directly in the next synthesis step without further purification (Supplementary Figure S2).

^{1}H-NMR (300 MHz, DMSO-d_6): δ (ppm) = 3.74 (d, 6 H, *J* = 7.5 Hz, OC***H***$_3$), 6.97 (s, 1 H, ArC***H***), 7.20 (s, 1 H, N***H***$_2$), 7.28 (s, 1 H, Ar-C***H***).

^{13}C-NMR (75 MHz, DMSO-d_6): δ (ppm) = 55.68, 56.20 (O***C***H$_3$), 102.35, 104.83 (Ar-***C***H), 121.30, 144.63 (Ar-***C***$_q$), 146.64, 148.19 (Ar-***C***–OCH$_3$), 165.81 (S–***C***=N).

IR (neat): ṽ [cm^{-1}] = 3366.63, 3309.42, 3088.76, 2994.78, 2962.09, 2933.48, 2761.86, 2157.98, 1650.40, 1601.36, 1535.98, 1470.60, 1433.83, 1401.14, 1352.10, 1307.15, 1196.82, 1164.13.

Melting point: 227 °C

FD-MS: [M] 210.6

Synthesis of intermediate I8:

In the same manner as that described for the preparation of **2**, starting from intermediate **I6** (90 mg, 0.3 mmol) and intermediate **I7** (71 mg,0.33 mmol), intermediate **I8** was obtained after precipitation and chromatography as solid (150 mg), which was used directly in the next synthesis step without purification (Supplementary Figure S2).

Synthesis of 6:

6 (14 mg, 0.031mmol, 15%, as a yellow solid) was obtained from intermediate **I8** (101 mg) and boron tribromide (1M in dichloromethane, 1.7 ml, 1.7 mmol) as described for the synthesis of **5** (Supplementary Figure S1 and Figure S2).

Melting point: 285 °C

FD-MS: [M] 444.0

^{1}H-NMR (300 MHz, DMSO-d_6) δ [ppm] = 12.21 (s, 1H), 9.73 (s, 2H), 9.18 (s, 2H), 7.77 (d, J=8.9 Hz, 2H), 7.71 (d, J=8.8 Hz, 1H), 7.50 (s, 2H), 7.33-7.20 (m, 3H), 7.15 (s, 1H), 7.10 (d, J=7.7 Hz, 2H), 6.89 (d, J=8.3 Hz, 1H)

^{13}C-NMR (75 MHz, DMSO-d_6) δ [ppm] = 164.22, 155.31, 155.16, 154.94, 152.61, 150.68, 145.63, 144.05, 141.88, 132.98, 131.91, 130.30, 128.76, 128.24, 128.14, 124.83, 122.94, 122.00, 120.60, 119.44, 117.52, 116.02, 108.86, 106.32.

FT-IR: $\tilde{\nu}$ [cm^{-1}] = 3533, 3277, 3072, 2355, 1643, 1602, 1538, 1299.

Synthesis of intermediate I9:

A solution of 1.0 eq. (498.5 mg, 2.010 mmol) of 2-iodobenzoic acid in 50 ml of ethyl acetate was cooled down to 0 °C in an ice water bath. 1.0 eq. (764.9 mg, 2.017 mmol) of (HBTU) and 2.0 eq. (0.7 ml, 4.236 mmol) of diisopropyl ethyl amine (DIPEA) were added and the reaction mixture was stirred at 0 °C for approximately one hour. Finally, 1.0 eq. (423.5 mg, 2.014 mmol) of compound **I7** was added and the reaction mixture was stirred at room temperature for several days. The organic layer was washed with saturated sodium hydrogen carbonate solution (3x), water (1x), an aqueous solution of 10% citric acid (3x), water (1x) and saturated sodium chloride solution (3x). The organic layer was dried over sodium sulfate, filtered and the solvent removed *in vacuo* [5]. The crude product was purified via column chromatography (silica gel) with a gradient of 100% dichloromethane to dichloromethane/methanol (39:1) and gave 786 mg (1.785 mmol, 89%) of the desired product **I9** as a light brown powder (Supplementary Figure S2).

^{1}H-NMR (300 MHz, $CDCl_3$): δ (ppm) = 3.77 (s, 3 H), 3.96 (s, 3 H), 6.56 (s, 1 H), 7.04 (td, 1 H, *J* = 7.7, 1.6 Hz), 7.18-7.25 (m, 2 H), 7.48 (dd, 1 H, *J* = 7.6, 1.5 Hz), 7.77 (d, 1 H, *J* = 7.9 Hz).

^{13}C-NMR (75 MHz, DMSO-d_6): δ (ppm) = 55.74, 55.97, 93.75, 103.62, 123.04, 128.08, 128.65, 131.79, 139.17, 140.53, 142.55, 147.14, 148.98, 156.18, 167.61.

IR (neat): ν̃ [cm^{-1}] = 3145.97, 3076.50, 2929.40, 2904.88, 2827.24, 2157.09, 1670.83, 1548.24, 1482.86, 1466.52, 1429.74, 1409.31, 1282.63, 1221.34, 1200.91, 1155.96, 1127.36.

Melting point: 184-185 °C

ESI-MS: $[M+H]^+$ 440.96, $[M+Na]^+$ 462.96, $[M+K]^+$, 478.95, $[2M+Na]^+$ 902.94

Synthesis of 7:

In a microwave reaction vessel (10 ml) containing a stirrer, 1.0 eq. (440.1 mg, 1.000 mmol) of **I9**, 1.0 eq. (0.14 ml, 1.022 mmol) of *p*-trifluoromethyl thiophenol and 2.0 eq. (276.8 mg, 2.002 mmol) of potassium carbonate were dissolved or suspended in isopropanol. After the addition of 2.0 eq. (0.12 ml, 2.152 mmol) of ethylene glycol and 0.1 eq. (19.6 mg, 0.103 mmol) copper(I) iodide the reaction mixture was irradiated in a synthesis microwave for up to three hours (method: closed vessel, power: 100-150 Watts, temperature: 80 °C). The reaction mixture was then poured into saturated sodium hydrogen carbonate solution and extracted with dichloromethane (3x). The combined organic layers were dried over sodium sulfate, filtered and the solvent was removed *in vacuo*. The crude product was purified via column chromatography (silica gel) with a gradient of 100% dichloromethane to dichloromethane/methanol (39:1) and gave 460 mg (0.938 mmol, 94%) of the desired product **7** as a dark brown solid (Supplementary Figure S2) [3].

^{1}H-NMR (300 MHz, $CDCl_3$): δ (ppm) = 3.75 (s, 3 H), 3.95 (s, 3 H), 6.83 (s, 1 H), 7.21 (dt, 2 H, *J* = 7.6, 3.0 Hz), 7.34 (qd, 4 H, *J* = 7.5, 1.3 Hz), 7.47 (d, 2 H, *J* = 8.5 Hz), 7.85 (dd, 1 H, *J* = 7.6, 1.5 Hz).

^{13}C-NMR (75 MHz, $CDCl_3$): δ (ppm) = 56.09, 56.49, 102.65, 102.88, 123.51, 126.31, 126.36, 128.02, 129.90, 131.35, 132.43, 133.00, 134.52, 134.72, 139.56, 141.80, 147.80, 149.36, 158.15, 165.46.

IR (neat): ṽ [cm^{-1}] = 3072.42, 2945.74, 2904.88, 2827.24, 1728.04, 1662.66, 1597.28, 1544.15, 1482.86, 1433.83, 1397.05, 1364.36, 1319.41, 1282.63, 1217.25, 1155.96, 1119.18.

Melting point: 194 °C

ESI-MS: $[M+H]^+$ 491.11, $[M+Na]^+$ 513.11, $[M+K]^+$ 529.09, $[2M+Na]^+$ 1003.24

Purity: 96%

Synthesis of 8:

8 (170mg, 0.368 mmol, 46%, as a yellow powder) was obtained from **7** (396 mg, 0.807 mmol) and boron tribromide (1M in dichloromethane, 2.8 ml, 2.8 mmol) as described for the synthesis of **5**.

^{1}H-NMR (300 MHz, DMSO-d_6): δ (ppm) = 7.11 (s, 1 H), 7.23 (s, 1 H), 7.36-7.49 (m, 3 H), 7.54 (dd, 2 H, *J* = 12.0, 6.7 Hz), 7.68 (d, 2 H, *J* = 8.2 Hz), 7.77 (d, 1 H, *J* = 7.8 Hz), 9.19 (d, 2 H, *J* = 4.1 Hz), 12.63 (s, 1 H).

^{13}C-NMR (75 MHz, DMSO-d_6): δ (ppm) = 106.38, 122.33, 125.93, 126.18 (2C), 127.08, 127.51, 128.30, 129.01, 130.30, 131.80, 133.28, 137.40, 141.52, 144.11, 145.69.

IR (neat): ṽ [cm^{-1}] = 3297.16, 3207.26, 3195.01, 3047.90, 2974.35, 2929.40, 2161.18, 1977.30, 1736.21, 1670.83, 1546.82, 1470.60, 1433.83, 1397.05, 1360.27, 1327.58, 1303.06, 1282.63, 1221.34, 1209.08, 1172.30, 1143.70, 1111.01.

Melting point: 223-224 °C

FD-MS: [M] 463.0

Purity: 97%

Quantum mechanics computations

The geometry optimizations of compound **3** resulted in two minima. Conformer 1 is energetically lower by 5.3 kcal/mol and is stabilized through intra-molecular π-π-interaction (Supplementary Figure S3A). Conformer 2 is also non-planar and features significantly twisted phenyl ring (Supplementary Figure S3B). Frequency calculations confirmed that both conformations are minima on the potential energy surface.

In order to evaluate whether the conformations obtained in the docking process are reasonable single point energy computations, as well as full and constrained geometry optimizations were performed. Single point energies cannot be compared to the energy of the minima obtained by the density functional (DFT) calculation directly, since the bond lengths and angles are too different. They can however be used to compare relative energies of the docking conformations. The lowest energy conformation is pose 3, while pose 2 and 1 are 1.5 and 5.3 kcal /mol, higher in energy (Supplementary Figure S3C).

The result of fully unconstrained optimizations of the docking poses as well as the docking conformations itself are shown as an overlay picture in (Supplementary Figure S3C). Optimizations of pose 1 lead to a very different structure and can thus not be used to judge the quality of pose 1. The optimized structures of pose 2 and 3 are however reasonably close to the original structures and are 7.4 and 1.2 kcal/mol higher in energy than conformer 1. These energy differences are so small that it can easily be surmounted by the interactions between inhibitor and enzyme.

In order to obtain estimations for pose 1 several constrained optimizations were performed, in which some dihedral angles were kept fixed, while all the other degrees of freedom were optimized. Constraining the dihedral angle between atoms 1-4 (Supplementary Figure S3) leads to structure that is 6.0 kcal/mol higher in energy than conformer 1. However, the plane of the amide group is rotated, so that it is in conjugation with the benzodiazole (Supplementary Figure 3D),

contrary to the structure of pose 1. The conjugation with the phenyl ring is also increased, although it stays twisted. Additionally constraining of the angles between atoms 5-4-6-7, 4-6-7-8 and 6-7-8-9 leads to a structure that is 18.3 kcal/mol above conformer 1 (Supplementary Figures S3D and S3E). Thus it can be concluded, that pose 1 is less favorable, which can be attributed to the fact, that the amid group is not in conjugation with the other aromatic rings.

Constrained optimizations with the same fixed dihedral angles of pose 2 and 3 lead to structures 15.8 and 4.6 kcal/mol higher in energy than the global minimum conformer 1. The higher energy of pose 2 can also be attributed to insufficient conjugation of the amid group, with the other aromatic rings.

Cartesian coordinates of compound 3

Conformer 1

O	0.881574	1.275439	-2.453903
C	1.597411	0.512018	-1.831164
N	1.096870	-0.609151	-1.182726
C	-0.241095	-0.886095	-0.972304
N	-0.590198	-1.812289	-0.125561
C	-1.966635	-1.886278	-0.042524
C	-2.674603	-0.980172	-0.875798
C	-4.065823	-0.917587	-0.873951
C	-4.733594	-1.791957	-0.017027
N	-6.208841	-1.749513	0.014690
O	-6.771158	-0.941892	-0.719281
O	-6.784262	-2.523557	0.772342
C	-4.064272	-2.702687	0.817967
C	-2.677476	-2.752407	0.806010
S	-1.535608	0.003779	-1.796921
C	3.086435	0.669302	-1.686034
C	3.919428	-0.330595	-2.208732
C	5.309672	-0.195710	-2.177067
C	5.876427	0.940131	-1.594265
C	5.058055	1.922592	-1.030293
C	3.660499	1.804944	-1.072892
S	2.704745	3.149794	-0.353586
C	1.449536	2.269120	0.588109
C	1.793617	1.262347	1.506617
C	0.795603	0.593939	2.213101
C	-0.547539	0.947467	2.029339
C	-1.621267	0.244328	2.816988
F	-2.805831	0.237850	2.163312
F	-1.837632	0.838633	4.014331
F	-1.292944	-1.044246	3.076694
C	-0.890568	1.961799	1.132604

C	0.104843	2.614962	0.402505
H	1.721143	-1.142630	-0.583604
H	-4.633738	-0.227840	-1.496100
H	-4.654127	-3.349083	1.465483
H	-2.126680	-3.432017	1.456307
H	3.466191	-1.209924	-2.673622
H	5.943745	-0.974331	-2.605664
H	6.961931	1.056409	-1.556440
H	5.502724	2.788880	-0.536191
H	2.842388	0.995926	1.651595
H	1.053750	-0.207882	2.906204
H	-1.939686	2.212943	0.973620
H	-0.163010	3.365242	-0.342168

Conformer 2

O	-0.208144	0.207078	-0.439457
C	0.547412	-0.745552	-0.555494
N	0.078330	-2.048134	-0.579408
C	-1.245689	-2.439288	-0.483106
N	-1.556395	-3.704134	-0.507125
C	-2.924830	-3.857957	-0.400624
C	-3.666107	-2.650826	-0.292048
C	-5.054710	-2.651004	-0.179655
C	-5.686920	-3.894275	-0.179900
N	-7.158767	-3.931703	-0.064307
O	-7.749163	-2.860471	0.033983
O	-7.701598	-5.031590	-0.074188
C	-4.985074	-5.107179	-0.285895
C	-3.600791	-5.091451	-0.396073
S	-2.569707	-1.268070	-0.323387
C	2.032793	-0.621451	-0.748193
C	2.597475	-1.147124	-1.923084
C	3.950506	-0.957954	-2.208469
C	4.756315	-0.253540	-1.308932
C	4.210496	0.244327	-0.123751
C	2.849339	0.072798	0.166517
S	2.219576	0.628135	1.767394
C	2.118147	2.408544	1.494442
C	2.763262	3.262846	2.400205
C	2.666366	4.646723	2.241287
C	1.938930	5.175157	1.170530
C	1.807845	6.667121	1.019310
F	1.638484	7.033534	-0.272265
F	0.742186	7.148939	1.704191
F	2.897311	7.321282	1.486962
C	1.300035	4.321282	0.263084
C	1.375671	2.938698	0.427855
H	0.740553	-2.818137	-0.621706
H	-5.646542	-1.741016	-0.094376
H	-5.547705	-6.039253	-0.279063
H	-3.027000	-6.015404	-0.479481
H	1.959810	-1.679430	-2.633394
H	4.372807	-1.357046	-3.133044
H	5.816824	-0.102043	-1.522480
H	4.840376	0.769031	0.596755
H	3.348764	2.843907	3.220757

H	3.172504	5.317085	2.937597
H	0.734732	4.741911	-0.569944
H	0.852294	2.265632	-0.252019

Pose 1 (docking structure)

N	36.139999	-10.125000	11.315000
N	34.222000	-11.845000	11.354000
N	30.906000	-13.340000	7.176000
C	37.445000	-10.551000	11.226000
C	35.070000	-10.938000	10.925000
C	33.313000	-12.342000	10.457000
C	33.442001	-11.789000	9.201000
C	32.678001	-12.080000	8.086000
C	31.690001	-13.028000	8.286000
C	31.495001	-13.632000	9.524000
C	32.304001	-13.287000	10.601000
C	38.431000	-9.456000	11.321000
C	38.859001	-8.803000	10.170000
C	39.786999	-7.772000	10.260000
C	40.287998	-7.393000	11.500000
C	39.860001	-8.046000	12.651000
C	38.931999	-9.077000	12.562000
C	39.930000	-10.555000	14.638000
C	39.918999	-11.295000	15.816000
C	41.111000	-11.811000	16.313999
C	42.299000	-11.580000	15.628000
C	43.605000	-12.142000	16.165001
C	42.305000	-10.839000	14.450000
C	41.115002	-10.321000	13.949000
O	37.873001	-11.685000	11.057000
O	29.875999	-12.676000	6.992000
O	31.287001	-14.264000	6.443000
F	44.231998	-11.284000	17.017000
F	44.514000	-12.428000	15.191000
F	43.432999	-13.301000	16.860001
S	34.723999	-10.674000	9.281000
S	38.397999	-9.894000	14.002000
H	35.904999	-9.208000	11.674000
H	32.828999	-11.638000	7.201000
H	30.771999	-14.313000	9.639000
H	32.159000	-13.724000	11.489000
H	38.498001	-9.075000	9.278000
H	40.095001	-7.302000	9.432000
H	40.955002	-6.651000	11.565000
H	40.221001	-7.773000	13.543000
H	39.060001	-11.456000	16.302000
H	41.113998	-12.345000	17.160000
H	43.164001	-10.679000	13.964000
H	41.112000	-9.788000	13.103000

Pose 2 (docking structure)

N	36.109001	-10.215000	11.569000
N	34.500999	-12.203000	11.257000
N	30.594999	-12.846000	7.381000
C	37.345001	-10.702000	11.929000

C	35.102001	-11.050000	11.073000
C	33.495998	-12.543000	10.389000
C	33.271999	-11.584000	9.426000
C	32.333000	-11.631000	8.413000
C	31.551001	-12.774000	8.394000
C	31.712999	-13.787000	9.332000
C	32.681999	-13.668000	10.323000
C	38.375000	-9.654000	12.069000
C	38.203999	-8.629000	12.994000
C	39.174000	-7.642000	13.125000
C	40.314999	-7.679000	12.332000
C	40.487000	-8.703000	11.408000
C	39.515999	-9.691000	11.276000
C	38.964001	-10.282000	8.661000
C	38.365002	-11.131000	7.735000
C	37.765999	-10.595000	6.599000
C	37.775002	-9.218000	6.404000
C	37.122002	-8.626000	5.165000
C	38.374001	-8.374000	7.332000
C	38.973999	-8.904000	8.469000
O	37.688000	-11.862000	12.117000
O	29.469000	-12.386000	7.616000
O	30.931999	-13.366000	6.308000
F	37.680000	-9.084000	4.010000
F	37.206001	-7.267000	5.105000
F	35.792999	-8.917000	5.081000
S	34.375999	-10.322000	9.719000
S	39.730999	-10.972000	10.118000
H	35.881001	-9.233000	11.657000
H	32.224998	-10.895000	7.744000
H	31.134001	-14.601000	9.295000
H	32.793999	-14.400000	10.996000
H	37.382999	-8.603000	13.564000
H	39.049999	-6.905000	13.790000
H	41.014000	-6.970000	12.427000
H	41.307999	-8.730000	10.837000
H	38.365002	-12.119000	7.886000
H	37.333000	-11.197000	5.928000
H	38.374001	-7.385000	7.182000
H	39.407001	-8.303000	9.141000

Pose 3 (docking structure)

N	35.824001	-11.538000	9.976000
N	38.276001	-10.866000	10.141000
N	41.175999	-9.734000	14.725000
C	34.742001	-11.772000	10.793000
C	37.043999	-11.169000	10.478000
C	39.153000	-10.554000	11.148000
C	38.577000	-10.612000	12.399000
C	39.194000	-10.353000	13.608000
C	40.528999	-10.000000	13.518000
C	41.183998	-9.917000	12.293000
C	40.494999	-10.193000	11.117000
C	33.629002	-12.466000	10.116000
C	33.193001	-13.701000	10.582000
C	32.145000	-14.355000	9.944000

C	31.532000	-13.773000	8.840000
C	31.968000	-12.538000	8.373000
C	33.016998	-11.885000	9.011000
C	34.818001	-10.815000	7.249000
C	36.127998	-10.383000	7.433000
C	37.108002	-10.752000	6.518000
C	36.765999	-11.549000	5.430000
C	37.832001	-11.958000	4.426000
C	35.455002	-11.979000	5.251000
C	34.472000	-11.612000	6.163000
O	34.584999	-11.462000	11.967000
O	42.372002	-9.415000	14.681000
O	40.513000	-9.835000	15.767000
F	38.421001	-10.888000	3.824000
F	37.355000	-12.736000	3.415000
F	38.844002	-12.672000	4.994000
S	36.952000	-11.064000	12.173000
S	33.563000	-10.339000	8.426000
H	35.759998	-11.639000	8.971000
H	38.712002	-10.416000	14.482000
H	42.148998	-9.659000	12.259000
H	40.971001	-10.132000	10.239000
H	33.632999	-14.119000	11.377000
H	31.830999	-15.243000	10.280000
H	30.778000	-14.243000	8.381000
H	31.528000	-12.120000	7.578000
H	36.362999	-9.810000	8.218000
H	38.051998	-10.447000	6.641000
H	35.220001	-12.552000	4.466000
H	33.528000	-11.918000	6.041000

Pose 1 full optimization

N	-0.527273	1.903326	-0.676123
N	-2.286815	0.519766	-0.035438
N	-3.737439	-4.849268	-0.860978
C	0.713954	2.122787	-1.248952
C	-1.244304	0.727214	-0.791785
C	-2.745711	-0.770605	-0.208078
C	-2.015285	-1.556875	-1.139444
C	-2.320442	-2.896466	-1.368668
C	-3.390376	-3.429734	-0.650619
C	-4.142835	-2.678561	0.268997
C	-3.821309	-1.346055	0.493095
C	1.551131	3.213717	-0.643168
C	2.238961	4.024714	-1.560138
C	3.067962	5.060143	-1.131583
C	3.254206	5.269446	0.237637
C	2.627077	4.434150	1.164131
C	1.766409	3.407202	0.742911
C	1.152118	0.743406	1.586509
C	0.131899	-0.132118	1.988043
C	0.180018	-1.476034	1.617962
C	1.237076	-1.944909	0.833873
C	1.227155	-3.357267	0.316122
C	2.270226	-1.079417	0.457148
C	2.238091	0.260424	0.840850

O	1.100672	1.474306	-2.209641
O	-3.073880	-5.482882	-1.675319
O	-4.669702	-5.308930	-0.208739
F	2.467679	-3.893059	0.279978
F	0.748441	-3.414271	-0.958038
F	0.447492	-4.170930	1.058904
S	-0.718504	-0.597076	-1.847436
S	0.984185	2.468939	2.073902
H	-0.801252	2.464051	0.128953
H	-1.752104	-3.526659	-2.049463
H	-4.963382	-3.165194	0.793672
H	-4.378892	-0.739416	1.208121
H	2.100167	3.822507	-2.623612
H	3.575654	5.692130	-1.862905
H	3.911596	6.067208	0.590642
H	2.814076	4.564164	2.231856
H	-0.726397	0.245048	2.546051
H	-0.627277	-2.150442	1.904446
H	3.098247	-1.452818	-0.147084
H	3.038689	0.934337	0.533407

Pose 2 full optimization

N	0.086211	0.632606	1.797499
N	-1.125303	-1.218100	0.904933
N	-5.497597	-1.731118	-2.595605
C	1.275869	-0.007405	2.199344
C	-0.951129	0.048809	1.095011
C	-2.207899	-1.434206	0.076746
C	-2.898566	-0.272818	-0.366400
C	-3.980494	-0.343877	-1.237454
C	-4.364085	-1.617624	-1.657214
C	-3.712824	-2.788538	-1.236418
C	-2.634375	-2.698402	-0.364888
C	2.347130	0.991924	2.556433
C	2.097261	1.916325	3.582173
C	3.087934	2.807292	4.005279
C	4.337540	2.791553	3.379141
C	4.585452	1.903646	2.327690
C	3.602626	0.992801	1.909079
C	2.583218	-0.114903	-0.458178
C	2.007234	-1.334306	-0.838281
C	0.907872	-1.347600	-1.699550
C	0.365539	-0.144866	-2.159273
C	-0.784991	-0.156330	-3.129816
C	0.921898	1.078000	-1.758623
C	2.034935	1.094170	-0.918421
O	1.420131	-1.205031	2.240619
O	-6.059304	-0.694962	-2.938088
O	-5.811226	-2.854103	-2.975865
F	-0.354692	-0.091057	-4.411602
F	-1.614968	0.901784	-2.948546
F	-1.533799	-1.278175	-3.024270
S	-2.130899	1.154083	0.313753
S	4.048464	-0.137860	0.583886
H	0.142882	1.643864	1.739206
H	-4.509364	0.531908	-1.608429

H	-4.068264	-3.747451	-1.610217
H	-2.101925	-3.586349	-0.021355
H	1.120784	1.909307	4.074304
H	2.883456	3.506769	4.818567
H	5.120188	3.486048	3.693451
H	5.548234	1.920342	1.812136
H	2.399831	-2.267143	-0.432610
H	0.448245	-2.293683	-1.987399
H	0.484872	2.012212	-2.114889
H	2.483898	2.042464	-0.615858

Pose 3 full optimization

N	-1.027182	-0.564751	0.828011
N	1.206775	0.026458	0.634748
N	5.280815	1.938098	3.999119
C	-2.239488	-0.727316	1.468979
C	0.152002	-0.119077	1.386915
C	2.265660	0.494032	1.384509
C	1.989323	0.705011	2.762792
C	2.963687	1.177581	3.638532
C	4.224667	1.435423	3.098801
C	4.529444	1.238632	1.740716
C	3.549088	0.766725	0.877502
C	-3.366951	-1.182492	0.577501
C	-4.042684	-2.340324	0.988303
C	-5.096135	-2.862058	0.235374
C	-5.502058	-2.213374	-0.933230
C	-4.861167	-1.038446	-1.336303
C	-3.793024	-0.512898	-0.593440
C	-1.606746	0.770063	-1.868892
C	-0.636357	1.787233	-1.836299
C	0.622787	1.566476	-2.383458
C	0.935242	0.326114	-2.953551
C	2.324891	0.102070	-3.481261
C	-0.029744	-0.680405	-3.005663
C	-1.305959	-0.458802	-2.477322
O	-2.365086	-0.588347	2.675071
O	6.385608	2.158070	3.513516
O	4.990362	2.106419	5.180073
F	2.654546	1.015137	-4.424843
F	2.480990	-1.121680	-4.028337
F	3.259195	0.221709	-2.499272
S	0.308325	0.283697	3.108180
S	-3.175687	1.118583	-1.068536
H	-0.959651	-0.729986	-0.174416
H	2.781972	1.348915	4.698309
H	5.536707	1.462646	1.393353
H	3.745964	0.602218	-0.182106
H	-3.727098	-2.824036	1.914729
H	-5.603423	-3.770542	0.566824
H	-6.328197	-2.610437	-1.527284
H	-5.195489	-0.505946	-2.228436
H	-0.859619	2.738096	-1.348313
H	1.380660	2.350452	-2.337131
H	0.212791	-1.641876	-3.459265
H	-2.059755	-1.247067	-2.524499

Pose 1 optimization with one constrained angle

S	0.000000	0.000000	0.000000
C	0.000000	0.000000	1.774821
N	1.154508	0.000000	2.378703
C	2.174010	0.013534	1.450034
C	1.761210	0.018539	0.090368
C	2.681820	0.033323	-0.955258
C	4.032924	0.044236	-0.606546
C	4.476180	0.039842	0.727730
C	3.546552	0.023981	1.759621
N	-1.166644	-0.008136	2.515216
C	-2.451560	-0.019566	2.004771
O	-2.659636	-0.087015	0.802033
N	5.035333	0.061079	-1.689349
O	6.219257	0.067164	-1.368969
O	4.624962	0.067531	-2.845775
C	-3.573539	-0.030335	3.005071
C	-4.632895	-0.904451	2.694932
C	-5.752833	-0.999797	3.516527
C	-5.840439	-0.200676	4.663242
C	-4.810542	0.685722	4.974133
C	-3.675983	0.789005	4.150920
S	-2.419992	2.005040	4.599973
C	-3.366885	3.529309	4.576570
C	-2.937199	4.570126	5.415964
C	-3.599851	5.796871	5.395382
C	-4.702466	5.984793	4.553849
C	-5.130882	4.947265	3.719169
C	-4.461353	3.723305	3.720632
C	-5.445678	7.291744	4.596063
F	-4.603587	8.345324	4.709993
F	-6.283674	7.351397	5.660148
F	-6.198821	7.490487	3.491588
H	-1.013831	-0.004524	3.518974
H	2.393828	0.038046	-2.005392
H	5.547283	0.048633	0.922332
H	3.857502	0.020761	2.805115
H	-4.554449	-1.499818	1.783999
H	-6.558302	-1.691452	3.261847
H	-6.713387	-0.265517	5.316524
H	-4.883131	1.326079	5.854570
H	-2.088450	4.418434	6.085965
H	-3.266467	6.610900	6.040949
H	-5.982081	5.102780	3.055288
H	-4.788568	2.921061	3.058496

Pose 1 optimization with four constrained angles

S	0.000000	0.000000	0.000000
C	0.000000	0.000000	1.787708
N	1.157326	0.000000	2.360423
C	2.171134	0.008795	1.420490
C	1.751551	-0.006621	0.061762
C	2.670302	-0.022704	-0.988052

C	4.018136	-0.015821	-0.640004
C	4.469364	0.004517	0.690382
C	3.543782	0.015881	1.724720
N	-1.226151	-0.009917	2.477341
C	-1.869537	1.165904	2.857125
O	-1.323791	2.249616	2.852979
N	5.018677	-0.031074	-1.729214
O	6.201354	-0.025911	-1.410220
O	4.600855	-0.049104	-2.881573
C	-3.323117	0.983730	3.235779
C	-4.298329	1.100587	2.232959
C	-5.654438	1.100014	2.560622
C	-6.046515	0.987820	3.898950
C	-5.084754	0.861881	4.901646
C	-3.719089	0.871523	4.579842
S	-2.472486	0.603758	5.857505
C	-2.714160	2.059229	6.889894
C	-2.920726	1.895169	8.265289
C	-3.043869	3.015938	9.090406
C	-2.976948	4.298529	8.539581
C	-2.761944	4.462511	7.164125
C	-2.619339	3.348267	6.340320
C	-3.170802	5.509889	9.412190
F	-2.868814	5.260662	10.706224
F	-4.454816	5.943970	9.388413
F	-2.405509	6.550163	9.010863
H	-1.808262	-0.835751	2.368232
H	2.382304	-0.037109	-2.037508
H	5.541262	0.010598	0.879214
H	3.856847	0.030815	2.769144
H	-3.987113	1.212994	1.191592
H	-6.404663	1.195502	1.773073
H	-7.106374	0.987683	4.162605
H	-5.386208	0.754467	5.944924
H	-2.986799	0.891585	8.688894
H	-3.199318	2.891271	10.162598
H	-2.685017	5.465629	6.742130
H	-2.417951	3.469323	5.274098

Pose 2 optimization with four constrained angles

S	0.000000	0.000000	0.000000
C	0.000000	0.000000	1.793545
N	1.154870	0.000000	2.373887
C	2.169132	0.015020	1.436517
C	1.757403	-0.008238	0.074864
C	2.674774	-0.028315	-0.971919
C	4.025030	-0.015367	-0.623040
C	4.469923	0.013509	0.707913
C	3.541296	0.027492	1.740873
N	-1.225514	-0.021849	2.448732
C	-1.535573	0.778053	3.574482
O	-0.706137	1.330333	4.252546
N	5.025479	-0.032535	-1.707924
O	6.208692	-0.018186	-1.388198
O	4.610862	-0.061904	-2.862046
C	-3.023593	0.837614	3.836480

C	-3.711404	-0.358009	4.096988
C	-5.067327	-0.345067	4.434460
C	-5.753879	0.868311	4.503924
C	-5.083182	2.064079	4.230043
C	-3.723111	2.061826	3.892214
S	-2.906792	3.637222	3.575280
C	-3.105026	3.853084	1.805414
C	-2.368082	4.902278	1.228410
C	-2.469540	5.166955	-0.135150
C	-3.299662	4.383321	-0.945189
C	-4.036535	3.341202	-0.373277
C	-3.944480	3.074994	0.993203
C	-3.376185	4.628161	-2.426486
F	-2.557198	3.798541	-3.119382
F	-3.019199	5.889745	-2.754175
F	-4.624373	4.421658	-2.908682
H	-2.023015	-0.240119	1.859169
H	2.388437	-0.049185	-2.021747
H	5.541129	0.023210	0.900935
H	3.852272	0.047928	2.785799
H	-3.168606	-1.305577	4.062984
H	-5.581660	-1.283539	4.651354
H	-6.812374	0.889359	4.771456
H	-5.613154	3.016912	4.273788
H	-1.709179	5.511065	1.851158
H	-1.897542	5.985468	-0.573524
H	-4.697886	2.738256	-0.997834
H	-4.537159	2.267786	1.424228

Pose 3 optimization with four constrained angles

S	0.000000	0.000000	0.000000
C	0.000000	0.000000	1.774644
N	1.155255	0.000000	2.376849
C	2.175572	0.026723	1.448202
C	1.762413	0.035149	0.089384
C	2.682866	0.058684	-0.955612
C	4.033067	0.074009	-0.606810
C	4.476801	0.066456	0.726056
C	3.547967	0.043101	1.757731
N	-1.168739	-0.014596	2.511809
C	-2.447638	-0.006011	1.985962
O	-2.646551	-0.089170	0.784372
N	5.034195	0.098695	-1.688882
O	4.622657	0.104335	-2.844876
O	6.217791	0.112319	-1.367950
C	-3.562896	0.304075	2.954104
C	-4.335416	1.436648	2.653186
C	-5.406019	1.807078	3.467247
C	-5.737221	1.030769	4.581032
C	-4.991710	-0.111936	4.878196
C	-3.897081	-0.477033	4.079949
S	-3.048201	-2.024682	4.448841
C	-1.674349	-1.521110	5.489237
C	-0.693230	-2.499107	5.739423
C	0.396504	-2.204109	6.550577
C	0.533620	-0.927543	7.115161

C	-0.435293	0.044723	6.867028
C	-1.541470	-0.247907	6.062074
C	1.732490	-0.632443	7.974996
F	2.887165	-0.725256	7.273958
F	1.837798	-1.510686	9.000505
F	1.688392	0.606714	8.510065
H	-1.024544	0.036267	3.518575
H	2.396836	0.064877	-2.006019
H	5.547840	0.079390	0.919803
H	3.859784	0.036933	2.802871
H	-4.088954	2.017493	1.762945
H	-5.990250	2.696450	3.222638
H	-6.583266	1.306198	5.214079
H	-5.256051	-0.739704	5.730556
H	-0.785371	-3.490536	5.291175
H	1.152172	-2.968187	6.740883
H	-0.335561	1.036229	7.309369
H	-2.302543	0.515833	5.896197

Buffers for DENV-2 and DENV-3 purification using HisTrap FF or GSTrap FF columns

DENV-2 lysis buffer: 50mM HEPES, 50mM NaCl, 5% Glycerol, pH 7.5

DENV-3 lysis buffer: 140mM NaCl, 2.7mM KCl, 10mM Na_2HPO_4, 1.8mM KH_2PO_4, 5mM DTT, pH 7.3

HPLC-based enzyme assay

In order to confirm PI activity for compounds bearing nitro groups (e.g. **2**, **3**), which may lead to false positive results due to quenching of the AMC fluorescence, the peptide cleavage and its inhibition by the compounds was analyzed by HPLC using a Phenomenex HyperClone 5 µm C18 120A column. PR assays were performed as described above for DENV-2 PR. Reactions with or without inhibitor (final concentration 50 µM, 200 µl each) were stopped by the addition of 400 µl acetonitrile. 100 µl of the resulting reaction mixtures were loaded onto the HPLC column and eluted with potassium phosphate buffer (25 mM KH_2PO_4/K_2HPO_4, pH 6.1) / methanol. Amounts of AMC (18 min retention time) produced and of residual substrate (10.5 min retention time) were detected and quantified at 347 and 326 nm, respectively. The percentage of inhibition by the compounds was calculated for each experiment comparing the integrals of the substrate

peaks without enzyme, after 30 min incubation of substrate and enzyme or after incubation of substrate, enzyme and inhibitor. For control also the integrals of the AMC peaks after 30 min incubation of substrate and enzyme were compared to those obtained after 30 min incubation of substrate, enzyme and inhibitor. Each experiment was performed in duplicates.

References

1. Moon, J.-K.; Park, J.-W.; Lee, W. S.; Kang, Y.-J.; Chung, H.-A.; Shin, M.-S.; Yoon, Y.-J.; Park, K.-H., Synthesis of some 2-substituted-thioxanthones. *Journal of Heterocyclic Chemistry* **1999,** *36*, 793-798.
2. (a) Punna, S.; Meunier, S.; Finn, M. G., A hierarchy of aryloxide deprotection by boron tribromide. *Organic letters* **2004,** *6* (16), 2777-9; (b) McOmie, J. F. W.; Watts, M. L.; West, D. E., Demethylation of aryl methyl ethers by boron tribromide. *Tetrahedron* **1968,** *24*, 2289-2292.
3. (a) Kwong, F. Y.; Buchwald, S. L., A General, Efficient, and Inexpensive Catalyst System for the Coupling of Aryl Iodides and Thiols. *Org. Letters* **2002,** *4* (20), 3517-3520; (b) Sperotto, E.; van Klink, G. P.; de Vries, J. G.; van Koten, G., Ligand-free copper-catalyzed C-S coupling of aryl iodides and thiols. *The Journal of organic chemistry* **2008,** *73* (14), 5625-8.
4. Stuckwisch, C. G., Derivatives of 2-Amino-6-methoxybenzothiazole. *J. Am. Chem. Soc.* **1949,** *71*, 3417-3417.
5. Kirin, S. I.; Wissenbach, D.; Metzler-Nolte, N., Unsymmetrical 1,n '-disubstituted ferrocenoyl peptides: convenient one pot synthesis and solution structures by CD and NMR spectroscopy. . *N. J. Chem.* **2005,** *29*, 1168-1173.

Supplementary Figures

Supplementary Figure S1. Syntheses of compounds (A) 1, (B) 2, (C) 3, (D) 4 and (E) 5.

Supplementary Figure S2. Syntheses of compounds (A) 6 and (B) 7 and 8.

Supplementary Figure S3. Quantum mechanics computations. (A) Conformer 1 and **(B)** 2 of compound **3** obtain from a global optimization. **(C)** Geometries obtained from unconstrained optimizations of Pose 1, 2, and 3. The docking poses are depicted in cyan while the optimized structures are shown in red. **(D)** Geometrical arrangements obtained from constrained optimizations of Pose 1. The docking poses are shown in cyan while the optimized structures are depicted in red. **(E)** Numeration of the atoms.

Supplementary Figure S4. Microscale Thermophoresis (MST) of compound 6. (A) Binding of compound **6** to DENV-2 PR in standard treated capillaries: shape of the MST curves (inset) and the resulting binding curve. From the resulting binding curve a K_D of 15.2 ± 0.61 µM was calculated. The fit quality is 0.98. **(B)** Binding of compound **6** to DENV-3 PR in standard treated capillaries. From the resulting binding curve a K_D of 3.77 ± 0.107 µM was calculated. The fit quality is 0.84.

Supplementary Figure S5. Cellular toxicity. Vero cells were incubated with PIs at the concentrations indicated in independent triplicates. The MTS substrate was added after 3 days. After incubation for 90 min the OD_{400} was measured. The OD_{400} of the DMSO was set to 100%. Compound numbers are indicated below the panel. Error bars represent the standard deviation. The experiment was repeated 3 times. The first bar represents the DMSO control.

Supplementary Figure S6. Inhibition of the DENV PR in cell culture PR assays. HEK 293T cells were transfected with the PR reporter plasmid and a DENV-2 PR expression construct. Decreasing concentrations of the compounds were added and the cells were incubated for 2 d.

Reporter cleavage was monitored by Western blotting using anti-GFP antibodies. Each sample was analysed on three independent Western blots and all experiments were repeated 3 times. Compound numbers are indicated below the panel. The first bar represents the substrate without PR. Bars represent the mean of all experiment. Error bars indicate the standard deviation. Significant differences in comparison to the substrate alone were indicated with one (p-value < 0.05) or two asterisks (p-value < 0.01) above the columns.

Supplementary Figure S7. The DENV PR cleaves GFP. HEK 293T cells were transfected with GFP (lanes 2 and 3), DsRed (lanes 4 and 5) or GFP-CS-DsRed reporter (lanes 6 and 7) construct with (lanes 1, 3, 5, 8) or without the DENV-2 PR (lanes 2, 4, 6). The processing was visualized by Western blotting using a anti-GFP antibody. Processing of GFP leads to a double band. Positions of the size markers are indicated.

Supplementary Table S1: Synthesized and tested derivatives

Structures	Inhibition at 50 µM
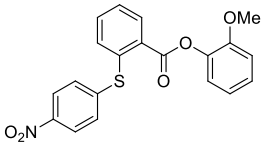	No inhibition
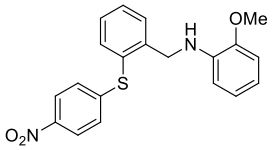	20 %
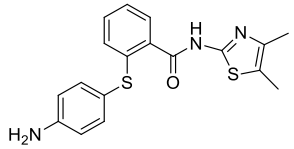	10 %
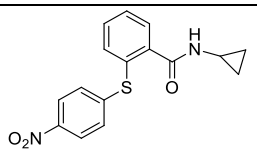	27 %

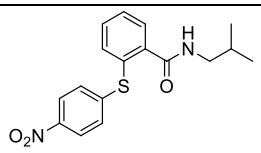	38 %
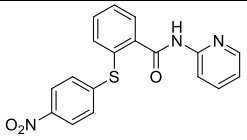	21 %
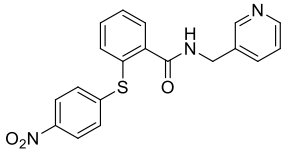	No inhibition
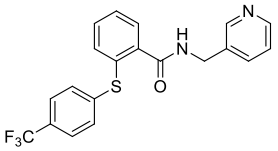	No inhibition
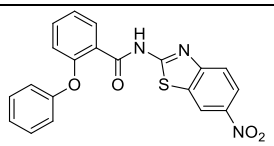	32 %
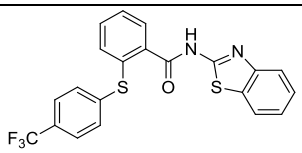	No inhibition
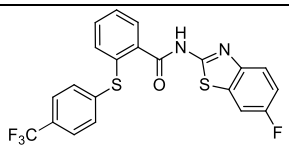	No inhibition
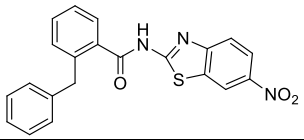	60 %
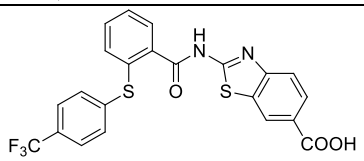	16 %
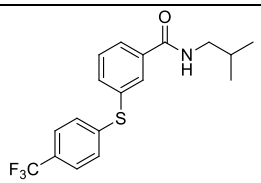	10 %
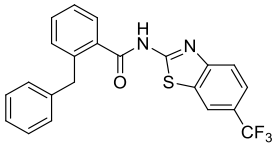	10 %

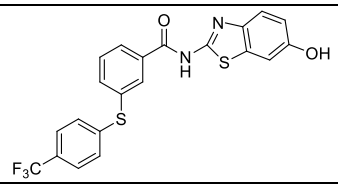	40 %
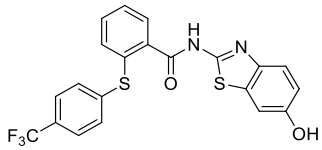	26 %
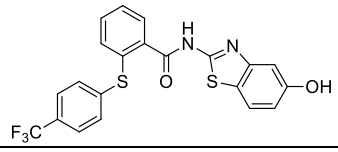	59 %

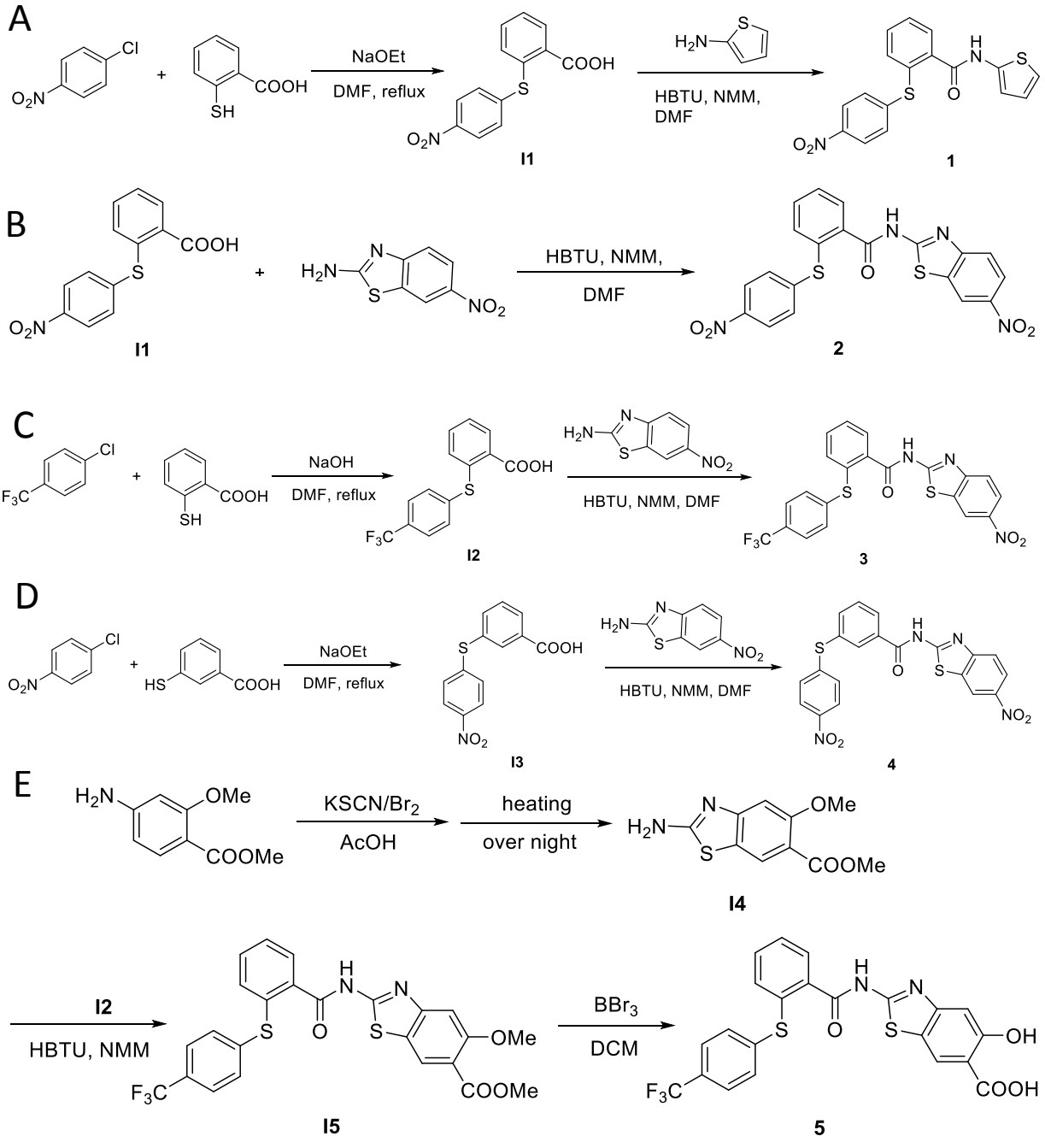

Supplementary Figure S1

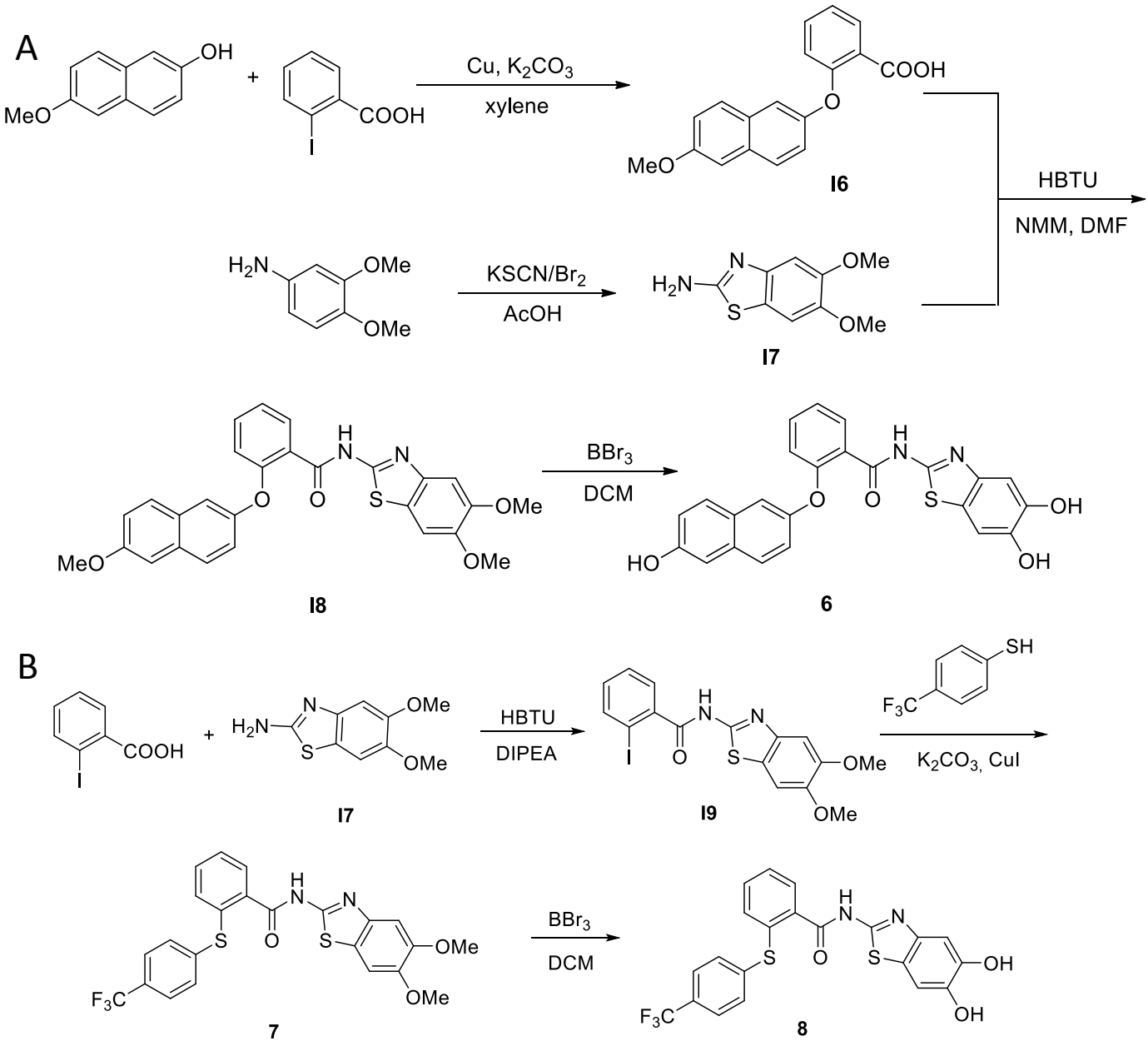

Supplementary Figure S2

A

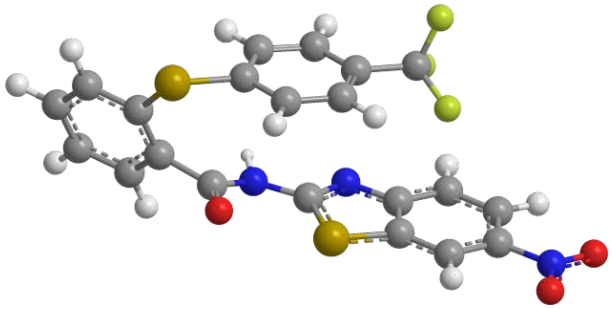

B

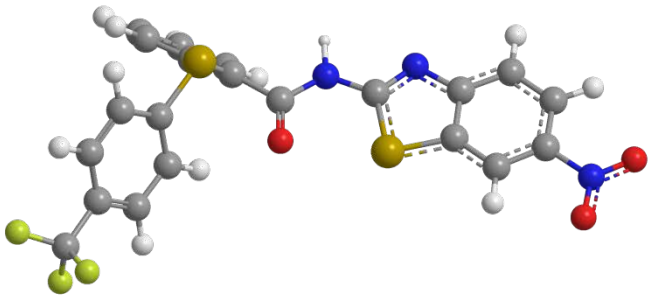

C

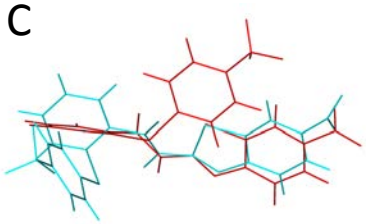

Pose 1

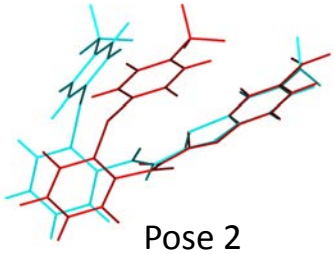

Pose 2

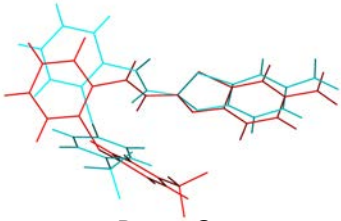

Pose 3

D

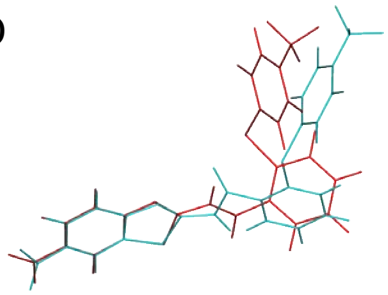

Pose 1 overlay 1
constrained angle

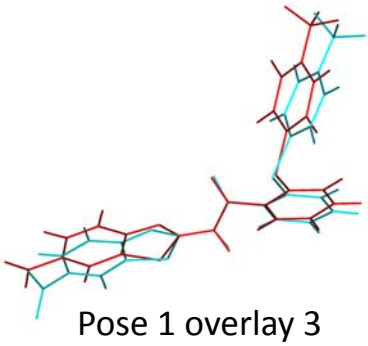

Pose 1 overlay 3
constrained angles

E

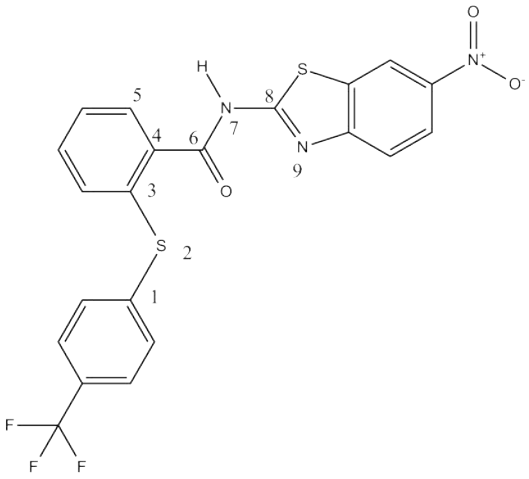

Supplementary Figure S3

A

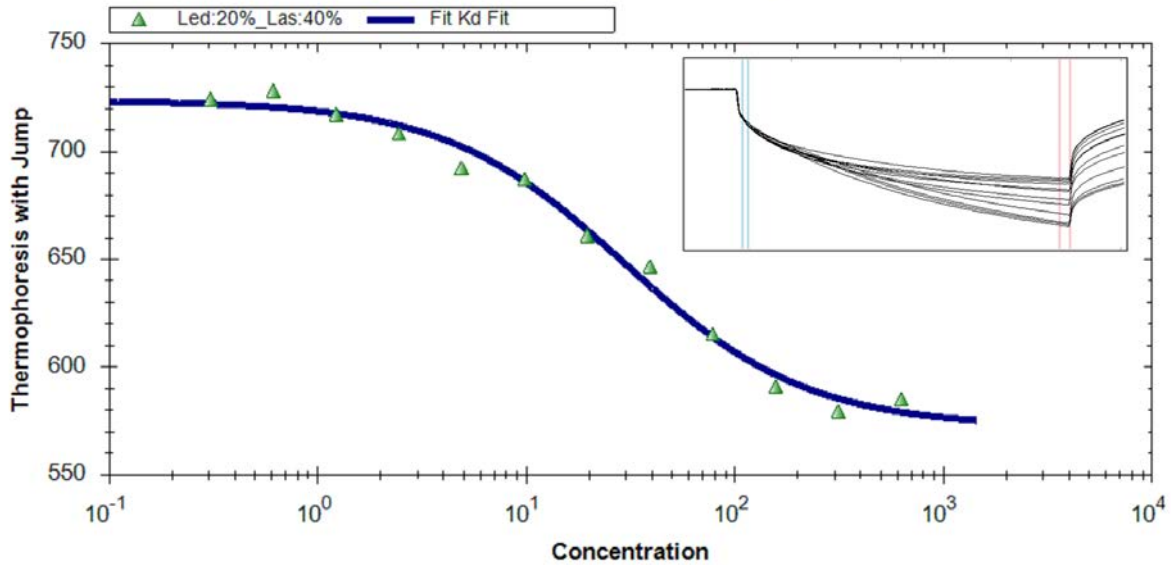

B

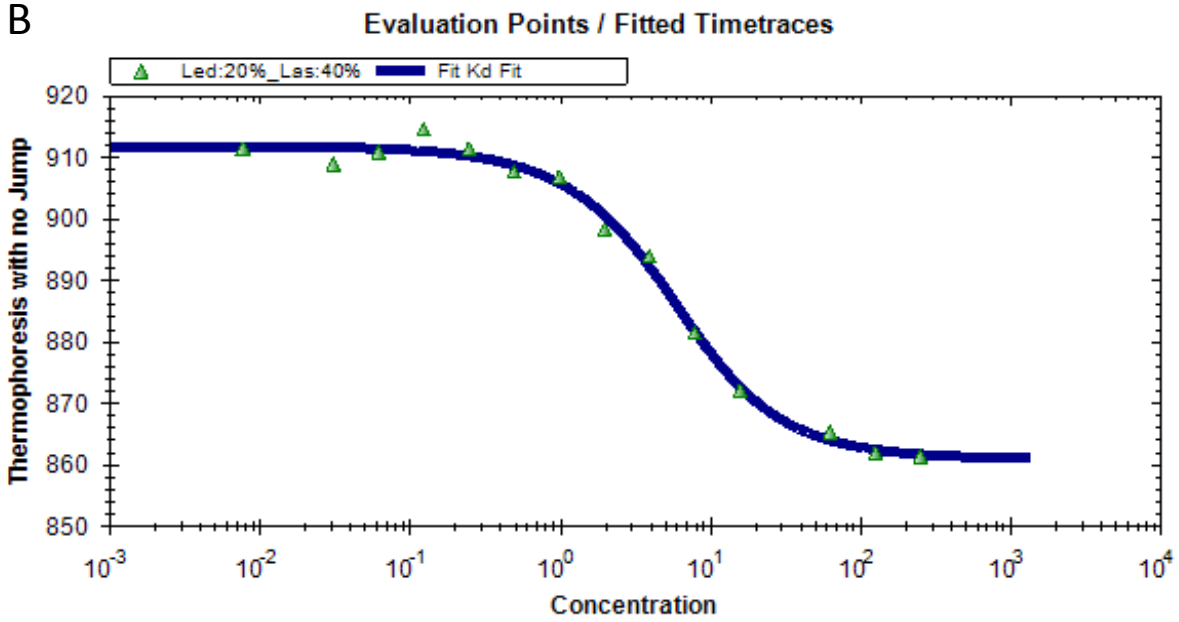

Supplementary Figure S4

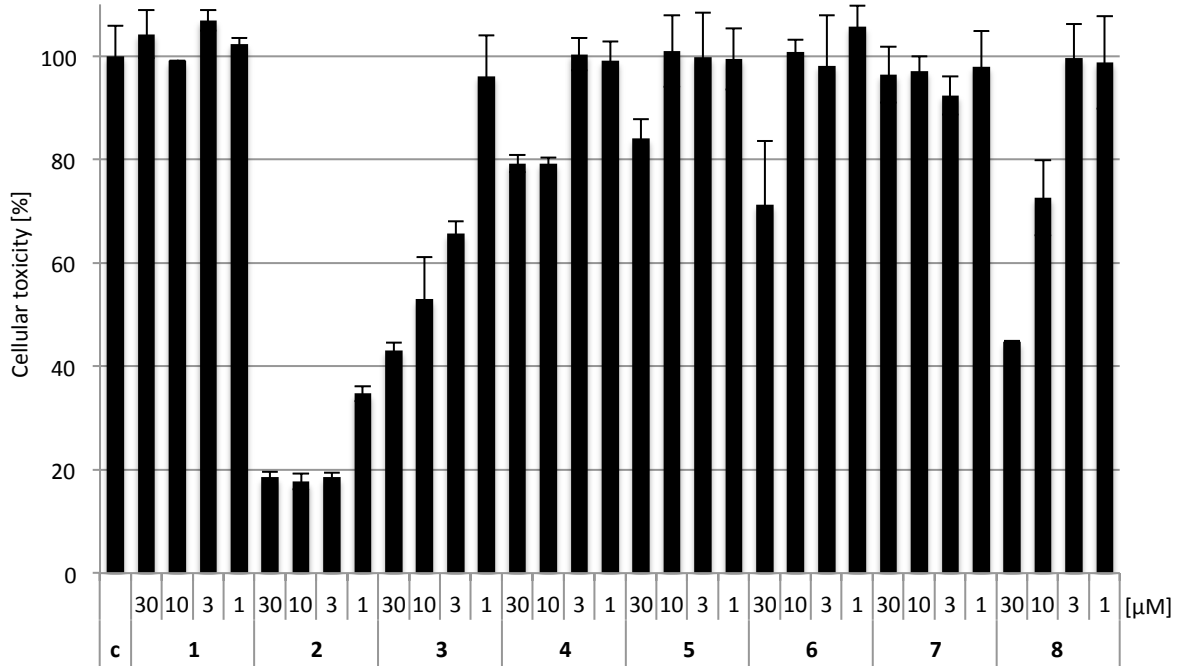

Supplementary Figure S5

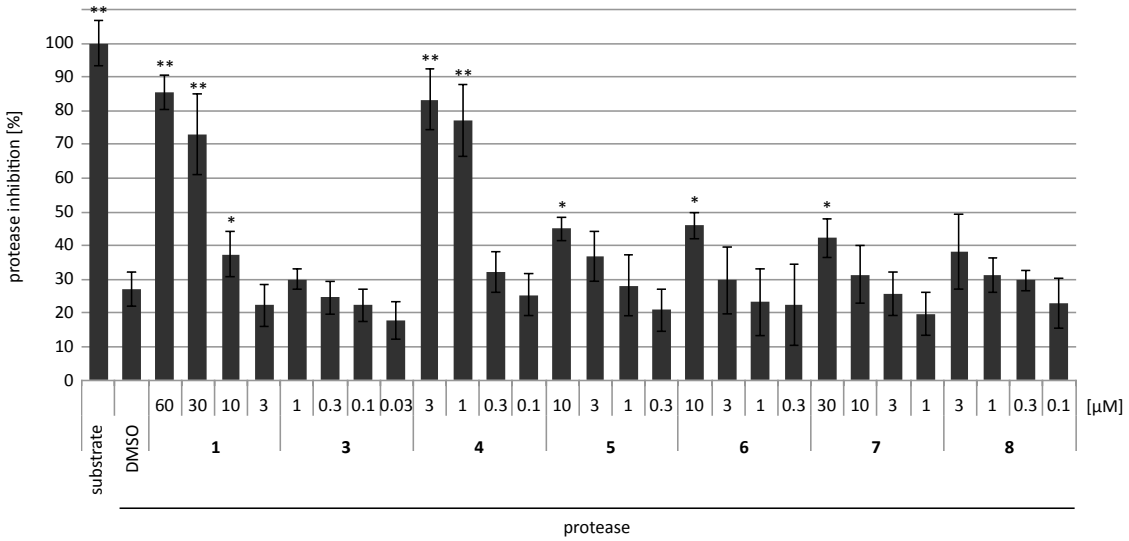

Supplementary Figure S6

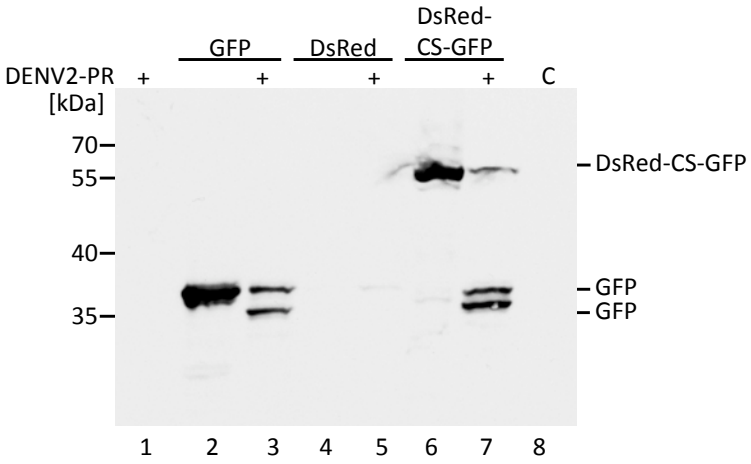

Supplementary Figure S7